3 August 2001

ELSEVIER

Chemical Physics Letters 343 (2001) 315–324

CHEMICAL PHYSICS LETTERS

www.elsevier.com/locate/cplett

Electron dipole–dipole interaction in ESEEM of nitroxide biradicals

L.V. Kulik [a], S.A. Dzuba [a,b,*], I.A. Grigoryev [c], Yu.D. Tsvetkov [a]

[a] *Institute of Chemical Kinetics and Combustion, Russian Academy of Sciences, Institutskaya-3, 630090 Novosibirsk, Russia*
[b] *Novosibirsk State University, Pirogova-2, 630090 Novosibirsk, Russia*
[c] *Novosibirsk Institute of Organic Chemistry, Russian Academy of Sciences, Lavrentyev Ave. 9, 630090 Novosibirsk, Russia*

Received 23 March 2001; in final form 8 June 2001

Abstract

Fourier transform of the standard primary electron spin echo envelope modulation (ESEEM) of nitroxide biradicals in organic glass shows a peak ascribed to electron–electron dipole–dipole interaction. The dipolar couplings obtained in imidazoline biradical and double spin-labeled peptide Trichogin GA IV are in good agreement with pulsed electron–electron double resonance (PELDOR) data. The intensity of this peak is increased substantially in a new three-pulse relaxation-induced dipolar modulation enhancement (RIDME) experiment. This experiment involves the non-resonant partner spin in the formation of ESEEM via a relaxation-induced change of the local dipolar field experienced by the resonant spin. © 2001 Published by Elsevier Science B.V.

1. Introduction

Application of electron spin echo (ESE) to study distances between unpaired electrons in biradicals and radical pairs in organic randomly oriented solids is now of great interest. ESE provides information in the very important nanometer range of distances. Several approaches in ESE has been used so far: double electron–electron resonance (DEER or PELDOR) [1–10], $2+1$ method [11–13], multiple-quantum EPR [14,15], solid-echo and Jeneer–Broekaert sequences [16]. These approaches are based on the conventional two-pulse ESE, which is substantially modified. Sometimes the instrumentation and/or theoretical description become rather complicated.

However, the routine two-pulse electron spin echo envelope modulation (ESEEM) experiment is also capable of obtaining information on the electron spin–spin interactions in biradicals. This was demonstrated a long time ago [17] for $SO_4^- \cdots SO_4^-$ pairs stabilized in UV-irradiated $K_2S_2O_8$ single crystals. Recently, the same approach was successfully applied to spin-correlated radical pairs appearing after a light flash in photosynthetic preparations [18]. In these studies ([19] and references therein) a strong electron–electron modulation was obtained. For biradicals in thermal equilibrium, the theory developed in [17] predicts that the echo signal in the case of a complete microwave excitation by two 90° and 180° pulses separated by time interval τ is

* Corresponding author. Fax: +7-3832-342350.
E-mail address: dzuba@ns.kinetics.nsc.ru (S.A. Dzuba).

0009-2614/01/$ - see front matter © 2001 Published by Elsevier Science B.V.
PII: S0009-2614(01)00721-7

$$E(2\tau) = \frac{\Delta\omega^2}{R^2}\cos(A\tau) + \frac{B^2}{R^2}\cos(R\tau)\cos(A\tau) + \frac{B}{R}\sin(R\tau)\sin(A\tau), \tag{1}$$

where

$$A = -\frac{2}{3}D(3\cos^2\xi - 1) + 2J,$$
$$B = \frac{1}{3}D(3\cos^2\xi - 1) + 2J,$$
$$R = (\Delta\omega^2 + B^2)^{1/2},$$

and $\Delta\omega$ is the difference in resonance frequencies for the two spins in the absence of dipolar and exchange interactions, D represents the dipolar coupling, ξ is the angle between the line connecting the two species and the direction of the external magnetic field, J is the value of the spin-exchange interaction (half the singlet–triplet splitting). In the point dipole approximation D is connected with the interspin distance value by the simple relation

$$D/\mathrm{MHz} = -\frac{7.8 \times 10^4}{(r/A)^3}. \tag{2}$$

The theory recently developed by Hore and co-workers [20] contains results that support the validity of Eq. (1).

The expression in Eq. (1) can be simplified substantially as the terms proportional to $\cos(R\tau)$ and $\sin(R\tau)$ dephase quickly, so that they can safely be dropped when observing echo signals beyond $\tau \cong 100$ ns, the experimental dead time of common spin-echo spectrometers. So, the echo amplitude is simply

$$E(2\tau) = \frac{\Delta\omega^2}{R^2}\cos\left\{(2J - \frac{1}{3}D(3\cos^2\xi - 1))2\tau\right\}. \tag{3}$$

One can see that the ESE is modulated with the frequency $2J - \frac{1}{3}D(3\cos^2\xi - 1)$. The cosine Fourier transform of Eq. (3) provides the Pake resonance pattern (Pake doublet).

In spite of the extreme simplicity of this approach, it was not used so far for organic biradicals in solids at thermal equilibrium. The obvious reason for that is the electron–nuclear hyperfine interactions, which strongly contribute to ESEEM of biradicals in solids [21]. It is therefore necessary to experimentally evaluate the relative importance of these two contributions.

The theory outlined above describes the case when the whole spectrum is excited uniformly by the microwave pulses. If only a fraction is excited the electron–electron modulation will appear only for the pairs in which both spins are involved. This is another restriction for the routine two-pulse experiment because the amplitude of the microwave field available in commercial ESE spectrometers is much smaller than the EPR linewidth of nitroxides widely used as spin labels in different applications.

The purpose of the present work is to demonstrate that, in spite of these restrictions, the simple two-pulse sequence in favorable cases may be applied to study electron–electron dipole–dipole interactions in organic biradicals in thermal equilibrium.

We also suggest a way to enhance the electron dipole–dipole contribution to ESEEM. This is done utilizing longitudinal relaxation of electron spins to increase the fraction of pairs contributing to ESEEM.

2. Experimental

The experiments were performed on a Bruker ESP 380E pulse X-band EPR spectrometer using a homemade rectangular resonator with a quartz dewar containing liquid nitrogen. The resonator quality

Table 1
Chemical structure of peptide Trichogin GA IV and its spin-labeled analogs

Trichogin GA IV	*n*Oct–Aib–Gly–Leu–Aib–Gly–Gly–Leu–Aib–Gly–Ile–Lol
PI	*n*Oct–Aib–Gly–Leu–Aib–Gly–Gly–Leu–TOAC–Gly–Ile–Leu–OMe
PII	*n*Oct–TOAC–Gly–Leu–Aib–Gly–Gly–Leu–TOAC–Gly–Ile–Leu–OMe

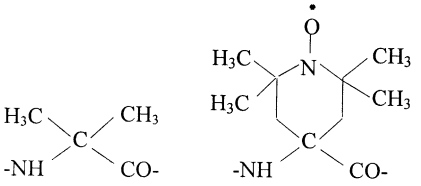

Aib TOAC

factor was adjusted to obtain the dead time of 72 ns. The lengths of the $\pi/2$ and π pulses in the two-pulse sequence were 8 and 16 ns, respectively. For the three-pulse sequence all pulse lengths were 16 ns with $\pi/2$ turning angles. Microwave excitation was applied at the central maximum of the nitroxide EPR spectrum. The influence of resonator ringing was removed by subtracting off-resonance time-domain data in each experiment.

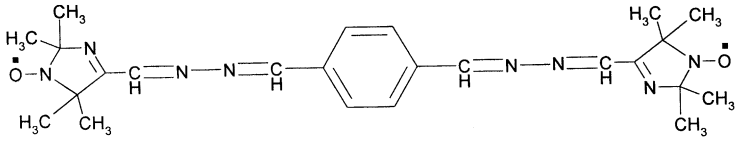

All experiments were performed at 77 K. A solution of imidazoline biradical in toluene was used at a concentration of 2 mM. The synthesis and purification of this biradical is described in [22]. Solution of nitroxide monoradical 2,2,6,6-tetramethyl-4-piperidone N-oxide (TEMPON) in toluene was used for comparative purpose. Spin labeled analogs of the peptide Trichogin GA IV (see Table 1) were dissolved in DMSO/chloroform 3:7 v:v mix. The peptides were obtained from Prof. Toniolo and co-workers; their synthesis is described in [23]. All samples were measured in a glassy state obtained by fast freezing at 77 K.

The time-domain traces of the primary ESEEM were acquired with a τ increment of 8 ns (350 points). Prior to Fourier transform the time-domain traces were zero-filled to 1024 points.

3. Results

3.1. Two-pulse ESEEM

The original time-domain ESEEM data for our samples is dominated by the electron–proton modulation. Primary ESEEM time-domain traces for the imidazoline biradical solution were extrapolated to zero τ value using a linear prediction method [24,25]. It was fitted by an exponential function, which was then subtracted before Fourier transformation. The resulting modulus Fourier spectrum is given in Fig. 1a. One

can see peaks around the single and double proton Larmor frequencies (14 and 28 MHz). In addition, a shallow but sharp negative peak with the minimum at 7.3 MHz is seen. This peak is absent for the spectrum of TEMPON in toluene obtained in the same way (Fig. 1b). This suggests that this negative peak is induced by electron dipole–dipole interaction representing the singularity ($\xi = \pi/2$) in the Pake spectrum. Its unusual shape we ascribe to interference of the weak electron–electron dipolar line with the huge wing of the electron–nuclear peak having a comparable intensity at this spectral position. This is readily supported by model calculation employing modulus Fourier transform of several damped harmonics differing in amplitudes [26].

The sign of the electron dipole–dipole peak in Fig. 1a may be corrected by dropping some initial data points of ESEEM time-domain traces prior to Fourier transform. Variation of initial τ value changes the relative phase of electron–electron and electron–nuclear contributions in the frequency spectrum. Fig. 1c presents the modulus ESEEM spectrum with $\tau_d = 72$ ns (which exactly corresponds to our experimental dead time). The Pake spectrum singularity appears now as a positive peak with the maximum at 7.1 ± 0.2 MHz. Numerical calculation with two damped harmonics (see above) indicates that the positive peak in the modulus Fourier transform spectrum obtained in such way reflects the correct value of the frequency of the weak harmonic.

The result of PELDOR experiments is shown in Fig. 1d (the original time-domain data were the same as shown in [2, Fig. 2]). In excellent agreement with the ESEEM results, it displays the peak at 7.15 MHz.

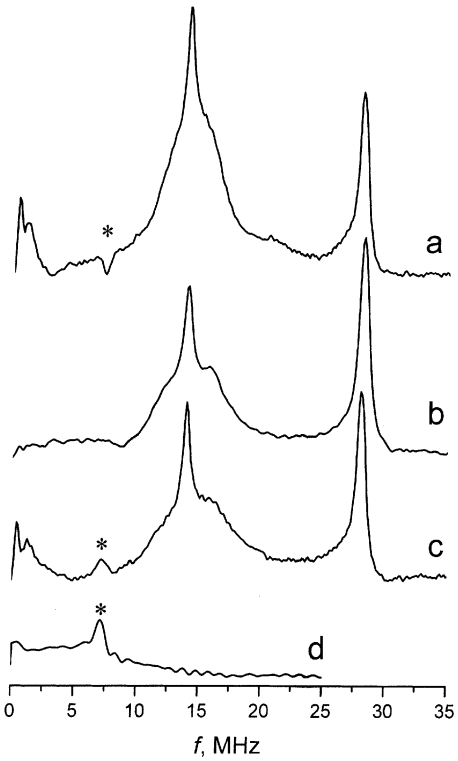

Fig. 1. Modulus ESEEM frequency spectra of imidazoline biradical (a), TEMPON (b), imidazoline biradical, initial time interval $\tau_d = 72$ ns is dropped (c), modulus spectra of imidazoline biradical PELDOR data (d). Asterisks mark the frequency position of the Pake spectrum singularity. Only the part of the spectrum corresponding to positive frequencies is shown.

To calculate the distance between two spins, we assumed that $J = 0$ because substantial overlap of the unpaired electron orbitals is not expected for the biradical of such structure. In this case the Pake spectrum singularity appears at the frequency $f_{\perp} = 2/3D$. The corresponding interspin distance calculated by Eq. (2) is 19.6 ± 0.2 Å.

We conclude that the routine two-pulse ESEEM can be used for precise determination of the interspin distance in nitroxide biradicals.

3.2. Suppression of electron–nuclear ESEEM

As the electron–electron and electron–nuclear contributions to ESEEM may be considered to be independent from one another, the pure electron–electron contribution may be obtained by dividing the biradical ESEEM by that of the monoradical of similar structure. This approach was applied to double spin-labeled peptide (see Table 1). We suggest that the second spin label does not influence substantially the surrounding of the first one. Ideally, the reference sample should contain 1:1 mix of the corresponding peptides labeled at the first and the second positions. We had at our disposal the peptide labeled at one position only (see Table 1) which nevertheless turned out to be adequate to suppress the electron–nuclear modulation.

The modulus two-pulse ESEEM spectrum of PII obtained by the same procedure as that for imidazoline biradical (without dead time recovery) does not show a noticeable electron–electron dipolar peak (Fig. 2a). This may be attributed to a distribution of the interspin distances in the biological sample, which results in weak peak intensity.

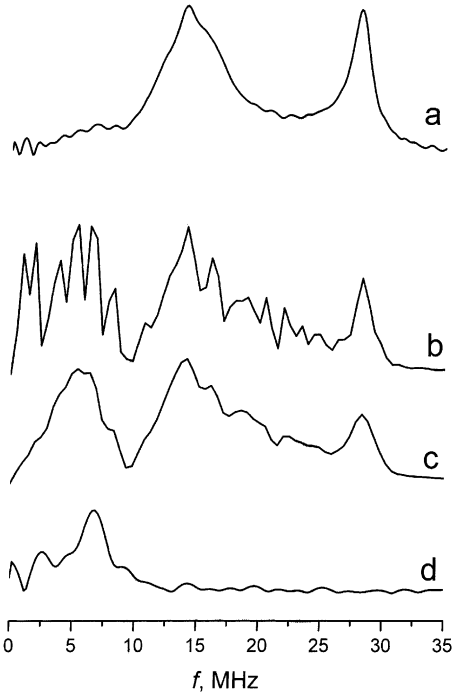

Fig. 2. Modulus ESEEM spectrum of double-labeled peptide PII (a), modulus spectrum of the time-domain traces obtained by dividing PII ESEEM by that of single spin-labeled peptide PI (see text), the apodization factor $a = 1$ MHz (b), $a = 2$ MHz (c), modulus spectrum of PII PELDOR data (d).

We recorded at the same conditions the two-pulse ESEEM of the monoradical PI sample. Special care was taken to keep the same microwave amplitude because its variation will result in different excitation degree of the electron–nuclear forbidden transitions. Then, the ESEEM time-domain trace for PII was divided by that for PI. To suppress the increasing noise in the tail of the decays, the result was multiplied by the apodization function $g = \exp(-(a\tau)^2)$, where a is the apodization factor. Then the result was fitted by the product of exponential and Gaussian decay functions, which was then subtracted. The modulus Fourier transform spectrum of the resulting data is shown at Fig. 2b for $a = 1$ MHz and in Fig. 2c for $a = 2$ MHz. In the latter case signal-to-noise ratio is acceptable. One can see that the additional broad peak with the maximum at 6.2 MHz appears. Its intensity is comparable with those of the electron–nuclear peaks at 14 and 28 MHz. We attribute this peak to electron dipole–dipole interactions. Its width is determined by the interspin distance distribution and Gaussian apodization. The mean interspin distance value obtained from the maximum frequency of this peak is 20.5 ± 1 Å. As in the previous case, $J = 0$ was suggested.

The PELDOR data (original time-domain data from [9, Fig. 5], was used for comparison. As the modulus Fourier transform spectrum of the original PELDOR data shows no sharp maximum, prior to performing Fourier transform we artificially introduced 'dead time' [21] by dropping the data corresponding to the initial 80 ns. The resulting modulus spectrum is shown in Fig. 2d. A clear maximum at 6.7 ± 0.4 MHz is seen. It gives the interspin distance of 20 ± 0.4 Å, in a reasonable agreement with the two-pulse ESEEM. The difference between the data may be explained by the broadening of the asymmetric singularity by the apodization, which is known to lead to a decrease in the peak frequency value [21].

This example demonstrates that two-pulse ESEEM may be used even for the unfavorable case of distributed interspin distances.

3.3. Relaxation-induced dipolar modulation enhancement

The very small intensity of the electron dipole–dipole peak seen in Fig. 1 is produced by relatively small excitation bandwidth. We estimated for our experiments a microwave amplitude of 7 G while the total width of the nitroxide EPR spectrum is 70 G. Only the fraction of pairs where both spins are excited by the microwave pulses contributes to dipolar modulation. We estimate this fraction as 15–20%. The experiment proposed below shows that this fraction may be increased substantially.

In this experiment a three-pulse stimulated echo sequence $\pi/2$–τ–$\pi/2$–T–$\pi/2$–τ– echo is used with fixed T and variable τ (see Fig. 3). This sequence is equivalent to the primary echo sequence with the only difference that the second pulse in the primary sequence is split into two halves. Let us consider a biradical in which

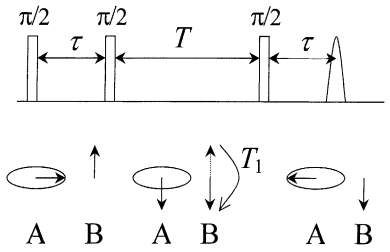

Fig. 3. Schematic representation of the RIDME experiment. Stimulated echo is measured as a function of time interval τ keeping fixedtime interval T. Spins A are excited by microwave pulses while spins B are not. During the evolution period T spin B flips due to spin–lattice relaxation. This leads to sudden alternation of the local dipolar field experienced by spin A. As a result, the non-resonant spins B also contribute to electron dipole–dipole ESEEM.

one electron spin (spin A) is excited by the microwave pulse and takes part in echo formation while the other (spin B) is not. Suppose that during the time interval T spin B flips under the action of longitudinal relaxation. This results, for an odd number of flips, in alternation of the local dipolar field experienced by spin A. So, during the first and the second τ interval the spin A precesses in different magnetic fields, with the difference determined by the electron–electron dipolar coupling. Thus, the echo intensity will be modulated with the same frequency as in Eq. (3). The fraction of spins B flipping an odd number of times is given by the relation

$$f_{\text{odd}} = \frac{1}{2}\{1 - \exp(-T/T_1)\}, \tag{4}$$

where T_1 is the spin–lattice relaxation time.

This method (relaxation-induced dipolar modulation enhancement (RIDME)) may be used as an alternative to pulsed ELDOR, in which the second microwave frequency is used to invert the partner spin. Up to the half of the pairs may be involved in formation of RIDME.

The simple interpretation presented for this phenomenon is valid only if $T_1 \gg \tau$. Also, the condition $T_1^2 A^2 \gg 1$ must hold otherwise the local dipolar field will alternate too rapidly to speak of a definite value at any chosen time moment. (Both these conditions are normally met for nitroxides in solids.) The theory of ESE in biradicals under conditions of spin–lattice relaxation, which may be employed in the general case, is given in [27]. For the three-pulse sequence this theory predicts the stimulated echo amplitude as

$$E(2\tau + T) = \left[\left(\mathrm{ch}Q\tau + \frac{1}{2T_1 Q}\mathrm{sh}Q\tau\right)^2 + \frac{A^2}{4Q^2}\mathrm{sh}^2 Q\tau \exp(-T/T_1)\langle \cos\theta^{(2)} \cos\theta^{(3)}\rangle_{g(\omega)}\right] \exp(-\tau/T_1), \tag{5}$$

where $Q^2 = 1/4T_1^2 - A^2/4$, $\theta^{(2)}$ and $\theta^{(3)}$ are the turning angles for the partner spins, for the second and third microwave pulses, respectively, $\langle \cdots \rangle_{g(\omega)}$ denotes averaging over the EPR line. It is assumed in (5) that $\Delta\omega^2 \gg B^2$.

Eq. (5) under the above conditions $T_1 \gg \tau$ and $T_1^2 A^2 \gg 1$, assuming also that the partner spins are truly B-spins (i.e. $\theta^{(2)} = \theta^{(3)} = 0$), is converted to

$$E(2\tau + T) = \frac{1}{2}\{1 + \exp(-T/T_1)\} + \frac{1}{2}\{1 - \exp(-T/T_1)\}\cos A\tau, \tag{6}$$

which is perfectly in line with the above simple consideration.

Fig. 4 presents the modulus RIDME spectra of the imidazoline biradical in toluene glass. The spectra were normalized to the same total signal intensity using the following procedure. Experimental time-domain traces (a τ increment of 8 ns, 250 points) were fitted by an exponential decay function, which was subtracted prior to Fourier transform. Then the resulted modulus spectra were divided by the initial amplitude of this exponential function.

It should be noted that no double nuclear frequency appears in this experiment, in contrast with the conventional two-pulse ESEEM. As follows from inspection of the relevant expression in [21], this harmonic is averaged during T period, if $2\pi\Delta f_N T > 1$, where Δf_N (≈ 1 MHz) is the nuclear peak linewidth. One can see in Fig. 4, that the intensity and the shape of the nuclear peak at 14 MHz is unchanged within the noise level when T is varied from 4.5 to 30 μs. This also follows from the above inspection.

The frequency position of the electron dipole–dipole peak in Fig. 4 is the same as that in Fig. 1 and does not change as T is varied. However, its intensity increases dramatically with increasing T. As described above, this effect may be explained by sudden jumps of the local dipolar field, due to longitudinal relaxation of electron spins. An odd number of electron spin flips will change the local dipolar field experienced by the partner spin. Some variation of the peak shape with increasing T may be attributed to interference with the nuclear peak.

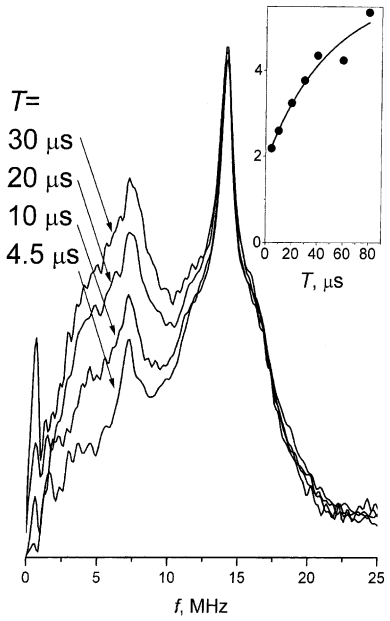

Fig. 4. Modulus ESEEM spectra obtained in three-pulse RIDME experiment (see Fig. 3) on imidazoline biradical at different T. Inset: the dependence of the relative intensity of the dipolar peak on T.

To verify this explanation, we have compared the time constant T_e of ESEEM enhancement with the electron spin–lattice relaxation time T_1. Inset in Fig. 4 shows the plot of relative intensity of electron dipolar peak vs T. The exponential fit results in $T_e = 50 \pm 25$ μs. The T_1 value was estimated from an inversion-recovery experiment (data not shown). Exponential fit of the initial 100 μs of inversion-recovery kinetic gave $T_1 = 60 \pm 10$ μs. (Because spectral diffusion also contributes to the recovery rate, T_1 estimated in such a way may be somewhat larger than its actual value.) We conclude that the T_e and T_1 timescales are close.

Exactly the same three-pulse RIDME experiment was performed on TEMPON in toluene. Neither peaks at the frequencies other then proton Larmor frequency nor the change of the spectra with T variation was found. It demonstrates that RIDME is a characteristic feature of biradicals.

4. Discussion

In this work we succeeded for the first time to detect the electron dipole–dipole interaction in biradicals in randomly oriented organic media with the routine two-pulse ESEEM. The method has both instrumental and theoretical simplicity. It is applicable when electron–electron and electron–nuclear anisotropic interaction are separated in the frequency domain. However, as compared with PELDOR and other recently developed methods, it is not free from the dead time problem.

To reduce the interfering electron–nuclear ESEEM, comparison with monoradicals is useful. However, as it is not always possible to prepare a sample with the corresponding monoradical, this approach is restricted to a certain class of compounds. The amplitude of electron dipole–dipole peaks may be substantially increased employing the proposed RIDME experiment based on the three-pulse stimulated echo sequence. The increase takes place because of relaxation-induced electron spin flips, which produce the

same effect on the dipolar coupling as microwave-induced electron spin flips in PELDOR. This approach works well at normal experimental conditions (nitroxide biradical at liquid nitrogen temperature). It may be also used for study of relaxation processes in biradicals.

It is interesting to note that the relative importance of the electron–electron and electron–nuclear interactions in ESEEM is completely different for thermally equilibrated biradicals and spin-polarized radical pairs. The result of this work shows that in the former case the electron–nuclear contribution prevails to a great extent. For the latter case the situation is perfectly opposite [18,19]. The explanation given in [28] suggests that in spin-polarized pairs the electron–nuclear transitions are also polarized so that the corresponding peaks in the frequency domain for the polyoriented sample average to zero.

Acknowledgements

The authors are grateful to A.J. Hoff for helpful discussions, A.D. Milov for presenting the original PELDOR time-domain data, A.V. Astashkin for providing the dead time recovery computer program, to A.G. Maryasov for drawing our attention to [27], and to C. Toniolo, F. Formaggio and M. Crisma for their gift of spin-labeled peptides. This work was supported by grants from Russian Foundation for Basic Research, numbers 00-15-97321 and 00-03-40124, from Ministry of Education of RF, number 2000.5.106, and from CRDF, number RC1-2056. INTAS Fellowship grant for Young Scientists, number YSF 00-99 is acknowledged by LVK.

References

[1] A.D. Milov, A.B. Ponomarev, Yu.D. Tsvetkov, Chem. Phys. Lett. 110 (1984) 67.
[2] A.D. Milov, A.B. Ponomarev, Yu.D. Tsvetkov, Zh. Struct. Khim. 25 (1984) 51.
[3] R.J. Larsen, D.J. Singel, J. Chem. Phys. 98 (1993) 5134.
[4] H. Hara, A. Kawamori, A.V. Astashkin, T. Ono, Biochim. Biophys. Acta 1276 (1996) 140.
[5] V. Pfannebecker, H. Klos, M. Hubrich, T. Volmer, A. Heuer, U. Wiesner, H.W. Spiess, J. Phys. Chem. 100 (1996) 13 428.
[6] R.E. Martin, M. Pannier, F. Diederich, V. Gramlich, M. Hubrich, H.W. Spiess, Angew. Chem. Int. Ed. 37 (1998) 2834.
[7] A.D. Milov, A.G. Maryasov, Yu.D. Tsvetkov, Appl. Magn. Reson. 15 (1998) 107.
[8] A.D. Milov, A.G. Maryasov, Yu.D. Tsvetkov, J. Raap, Chem. Phys. Lett. 303 (1999) 135.
[9] A.D. Milov, A.G. Maryasov, R.I. Samoilova, Yu.D. Tsvetkov, J. Raap, V. Monaco, F. Formaggio, M. Crisma, C. Toniolo, Dokl. Akad. Nauk 370 (2000) 265.
[10] M. Pannier, S. Veit, A. Godt, G. Jeschke, H.W. Spiess, J. Magn. Reson. 142 (2000) 331.
[11] V.V. Kurshev, A.M. Raitsimring, Yu.D. Tsvetkov, J. Magn. Reson. 81 (1989) 441.
[12] A.V. Astashkin, Y. Kodera, A. Kawamori, Biochim. Biophys. Acta 1187 (1994) 89.
[13] A.V. Astashkin, H. Hara, A. Kawamori, J. Chem. Phys. 108 (1998) 3805.
[14] S. Saxena, J.H. Freed, Chem. Phys. Lett. 251 (1996) 102.
[15] P.P. Borbat, J.H. Freed, Chem. Phys. Lett. 313 (1999) 145.
[16] G. Jeschke, M. Pannier, A. Godt, H.W. Spiess, Chem. Phys. Lett. 331 (2000) 243.
[17] V.F. Yudanov, K.M. Salikhov, G.M. Zhidomirov, Yu.D. Tsvetkov, Teor. Eksper. Khim. 5 (1969) 663.
[18] S.A. Dzuba, P. Gast, A.J. Hoff, Chem. Phys. Lett. 236 (1995) 595.
[19] S.A. Dzuba, A.J. Hoff, in: L.J. Berliner, S.S. Eaton, G.R. Eaton (Eds.), Biological Magnetic Resonance, Kluwer/Plenum, New York, 2000, p. 569.
[20] C.R. Timmel, C.E. Fursman, A.J. Hoff, P.J. Hore, Chem. Phys. 226 (1998) 271.
[21] S.A. Dikanov, Yu.D. Tsvetkov, Electron Spin Echo Modulation (ESEEM) Spectroscopy, CRC Press, Boca Raton, FL, 1992.
[22] I.A. Grigoryev, S.A. Dikanov, G.I. Schukin, L.B. Volodarskiy, Yu.D. Tzvetkov, Zh. Struct. Khim. 23 (1982) 59.
[23] P. Hanson, G. Martinez, G.L. Millhauser, J. Am. Chem. Soc. 118 (1996) 271.
[24] S.A. Dikanov, A.V. Astashkin, Yu.D. Tsvetkov, M.G. Goldfeld, Chem. Phys. Lett. 101 (1983) 206.
[25] R. De Beer, D. van Ormondt, in: A.J. Hoff (Ed.), Advanced EPR: Application to Biology and Biochemistry, Elsevier, Amsterdam, 1989.

[26] S. Van Doorslaer, G.A. Sierra, A. Schweiger, J. Magn. Reson. 136 (1999) 152.
[27] K.M. Salikhov, S.A. Dzuba, A.M. Raitsimring, J. Magn. Reson. 42 (1981) 255.
[28] S.A. Dzuba, Chem. Phys. Lett. 278 (1997) 333.